Organic Materials

Supporting Information
for DOI: 10.1055/s-0039-3401017

Georg Thieme Verlag KG, Rüdigerstraße 14, 70469 Stuttgart, Germany

Supporting Information

For

Small molecule donor/polymer acceptor type organic solar cells: effect of terminal groups of small molecule donors on optoelectronic properties

*Junhui Miao,[a,b] Bin Meng,[*a] Jun Liu[*a] and Lixiang Wang[a]*

[a] *State Key Laboratory of Polymer Physics and Chemistry, Changchun Institute of Applied Chemistry, Chinese Academy of Sciences, Changchun 130022, People's Republic of China. E-mail: mengbin@ciac.ac.cn; liujun@ciac.ac.cn*

[b] *University of Science and Technology of China, Hefei 230026, People's Republic of China.*

Contents

1. Experimental details

^{1}H NMR spectra were measured with a Bruker AV-400 MHz NMR spectrometer. ^{13}C NMR spectra were measured with a Bruker AV-500 MHz NMR spectrometer. Elemental analysis was recorded on a VarioEL elemental analyzer. Thermal analysis was performed on a Perkin-Elmer 7 instrument under nitrogen flow at a heating rate of 10 ^{o}C min^{-1}. Differential scanning calorimetry (DSC) was performed with a TA DSC Q2000 instrument under nitrogen at the heating and cooling rates of 10 ^{o}C min^{-1} in two heating/cooling cycles. Cyclic voltammetry (CV) were performed on a CHI660a electrochemical workstation using Bu_4NPF_6 (0.1 mol L^{-1}) in acetonitrile as electrolyte solution and ferrocene as an internal reference at a scan rate of 100 mV s–1. The CV cell consisted of a Pt wire counter electrode, a glassy carbon electrode, and a standard calomel reference electrode. The small molecules were casted on the working electrode for measurements. The ferrocene/ferrocenium (Fc/Fc+) was used as an internal standard, which was assigned an absolute energy of –4.80 eV. The highest occupied molecular orbital (HOMO) and the lowest unoccupied molecular orbital (LUMO) energy levels of the material were estimated by the equations: $E_{HOMO/LUMO}$ = –(4.80 + E_{onset}^{ox}/E_{onset}^{red}) eV. UV-vis absorption spectra were measured with a Perkin-Elmer Lambda 35 UV−vis spectrometer. Photoluminescence (PL) spectra were measured with a Horiba Jobin-Yvon FL3C-111 fluorescence spectrophotometer. The pure and blend films were prepared from chlorobenzene (CB) solution and annealed at 180 °C for 10 min. Atomic force microscopy (AFM) were performed with a SPA300HV (Seiko Instruments, Inc., Japan) in tapping mode. The thickness of films was measured by step profiler with a Dektak 6M Stylus Profile.

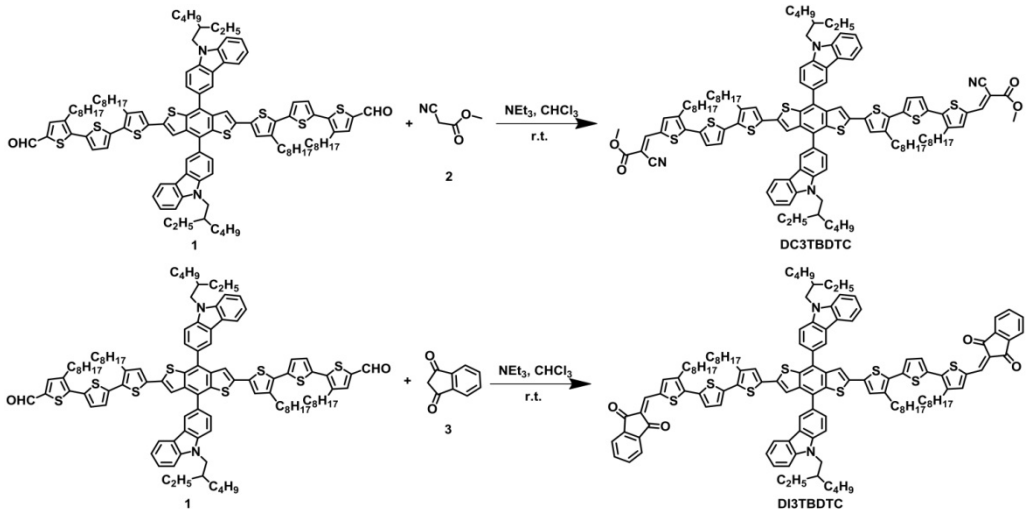

Figure S1. Synthetic routes of DC3TBDTC and DI3TBDTC.

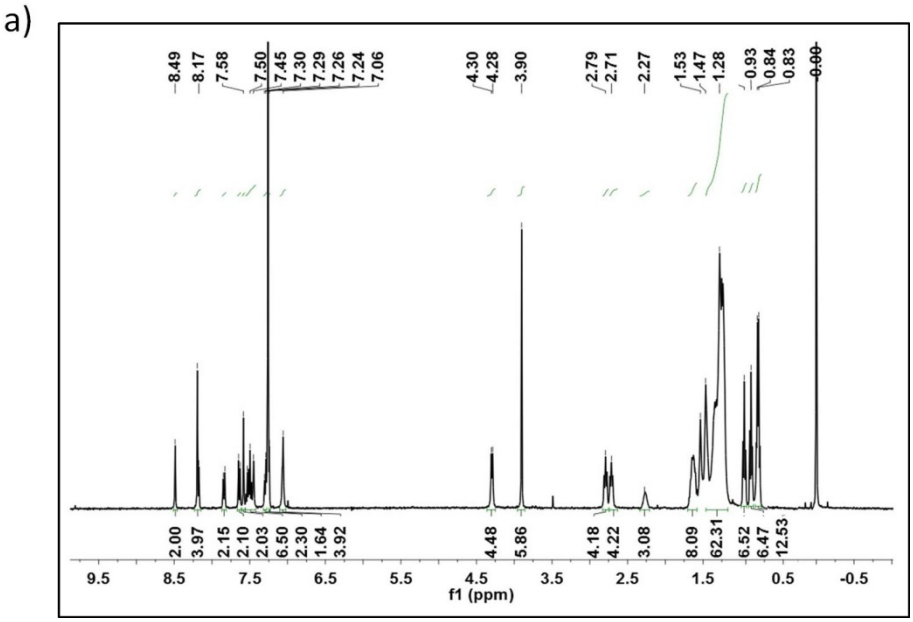

b)

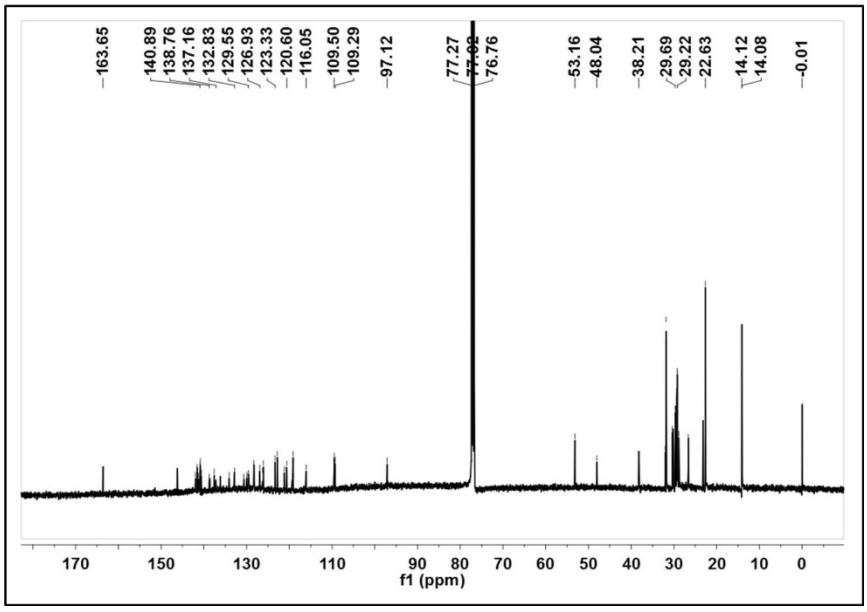

Figure S2. ^{1}H NMR and ^{13}C NMR of DC3TBDTC.

a)

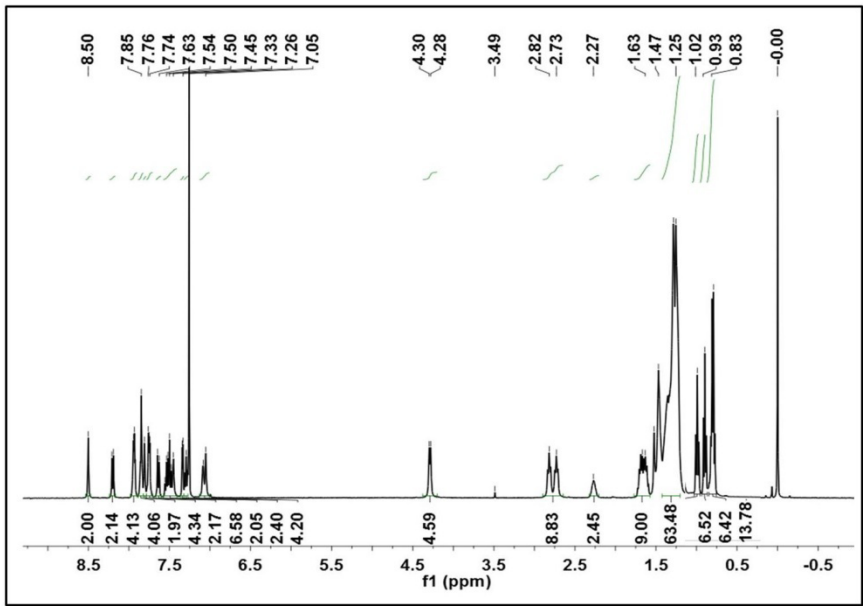

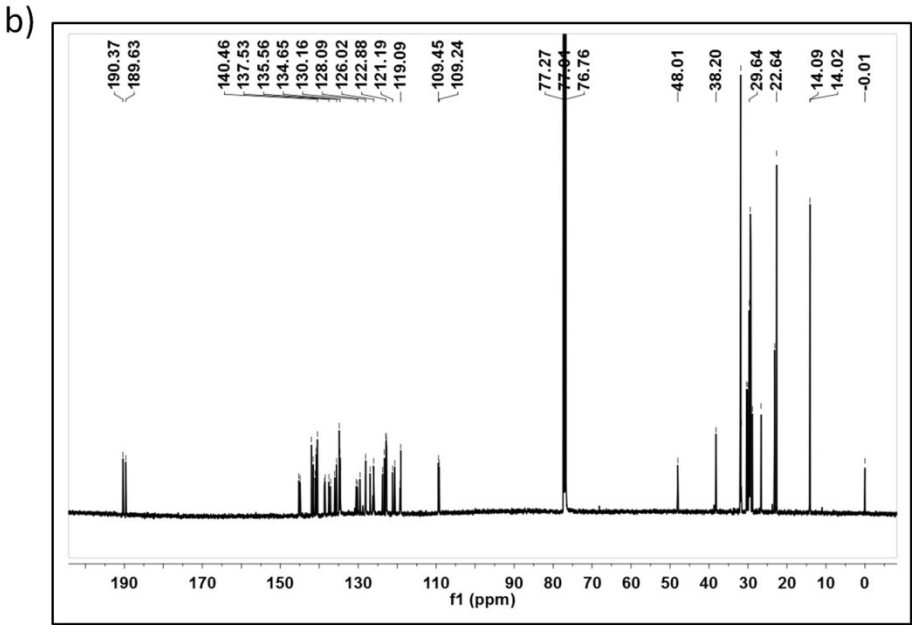

Figure S3. ^{1}H NMR and ^{13}C NMR of DI3TBDTC.

2. Thermal properties

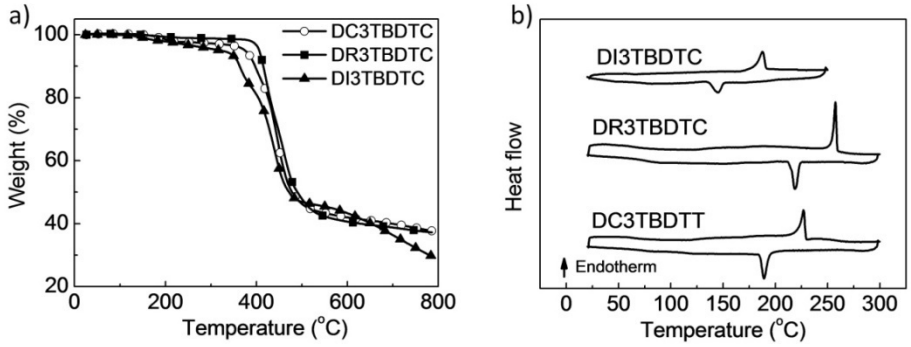

Figure S4. a) TGA curves and b) DSC curves of DC3TBDTC, DR3TBDTC and DI3TBDTC.

3. Density functional theory calculations

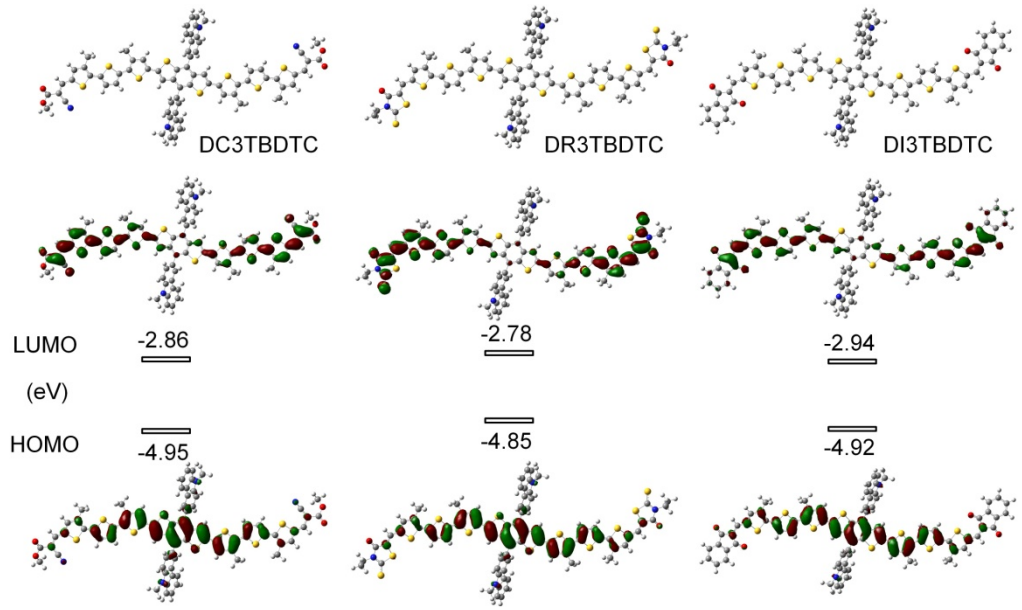

Figure S5. The geometry-optimized structure and molecular orbital surfaces of the LUMO and HOMO of DC3TBDTC, DR3TBDTC and DI3TBDTC, obtained at the DFT/B3LYP/6-31G* level with all the long alkyl chains have been replaced by methyl groups for simplification.

4. OSC device fabrication and measurement

The OSC devices were fabricated with the configuration of ITO/PEDOT:PSS/Active layer/LiF/Al. Polymer acceptor PBN-13 was synthesized in our laboratory with the number-average molecular weight (M_n) of 72500 and polydispersity index of 2.10. Indium tin oxide (ITO) glass substrates were cleaned by sequential ultrasonication in deionized water, acetone, and isopropyl alcohol, followed by drying at 120 °C for 30 min and treatment with UV-ozone for 40 min. PEDOT:PSS (Baytron PVP Al 4083) was spin-coated on the ITO glass substrates at 5000 rpm for 40 s to give a film thickness of 40 nm, followed by baking at 120 °C for 30 min. Then, the substrates were transferred to a nitrogen-filled glove box. The blends were spin-coated onto the PEDOT:PSS layers to produce the active layers. The blend ratio was 3:1 (w:w) for small molecule donor:polymer acceptor in CB solution. All of the active layers were annealed at 180 °C for 10 min. Finally, the active layers were transferred to a vacuum chamber, and LiF (5 nm) and Al (100 nm) were deposited by

thermal evaporation at the pressure of about 2×10^{-4} Pa. The active area of each device was 2 mm^2. The current density (J–V) curves of the OSC devices were measured using a computer-controlled Keithley 2400 source meter under 100 mW cm^{-2} AM 1.5G simulated solar light illumination provided by an XES-40S2-CE Class Solar Simulator (Japan, SAN-EI Electric Co., Ltd). The EQE spectra were measured using a Solar Cell Spectral Response Measurement System QE-R3011 (Enlitech Co., Ltd). The light intensity at each wavelength was calibrated using a calibrated monosilicon diode.

5. Hole/electron-only devices fabrication and hole/electron mobility measurement

The electron/hole mobilities were measured using space charge limited current (SCLC) method. The hole-only and electron-only device structures for the blend film are ITO/PEDOT:PSS/Active layer/MoO_3/Al and ITO/PEIE/ Active layer/MoO_3/Ca/Al, respectively. The current-voltage curves in the range of 0–8 V were recorded using a computer-controlled Keithley 2400 source meter, and the results were fitted to a space-charge limited function:

$$J = \frac{9}{8}\varepsilon_r\varepsilon_0\mu\frac{V^2}{L^3}\exp\left(0.89\beta\frac{\sqrt{V}}{\sqrt{L}}\right)$$

where J is the current density, ε_0 is the permittivity of free space, ε_r is the relative permittivity of 3 for molecules, μ is the zero-field mobility, V is the potential across the device ($V = V_{applied} - V_{bias} - V_{series}$), L is the thickness of active layer, and β is the field-activation factor. The series and contact resistance (V_{series}) of the device (10–15 Ω) were measured using blank device of ITO/PEDOT:PSS/MoO_3/Al or ITO/PEIE/Ca/Al. The range of 0–5 V was used to extract the mobility values.

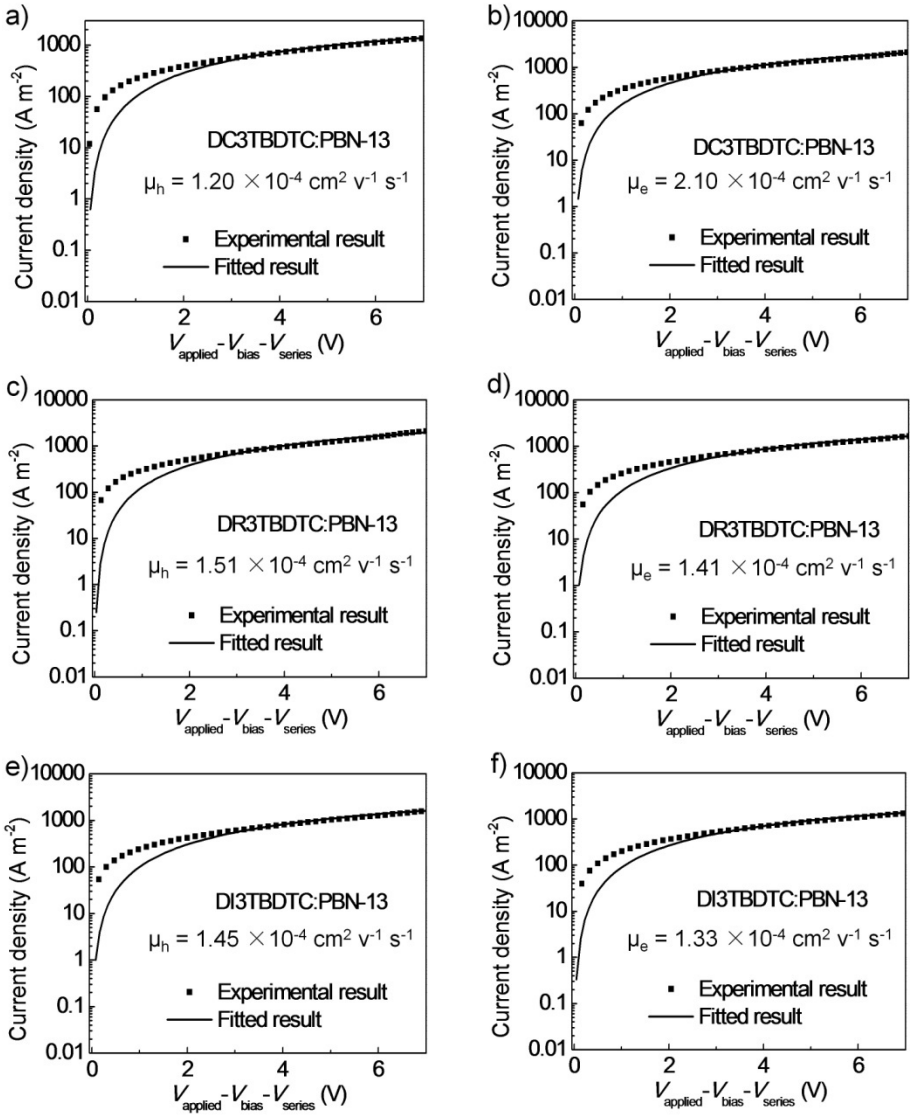

Figure S6. J–V curves and SCLC fittings of a, c, e) the hole-only device and b, d, f) the electron-only device based on the DC3TBDTC:PBN-13 blend, the DR3TBDTC:PBN-13 blend and the DI3TBDTC:PBN-13 blend, respectively.

6. Charge generation, collection and recombination behaviors

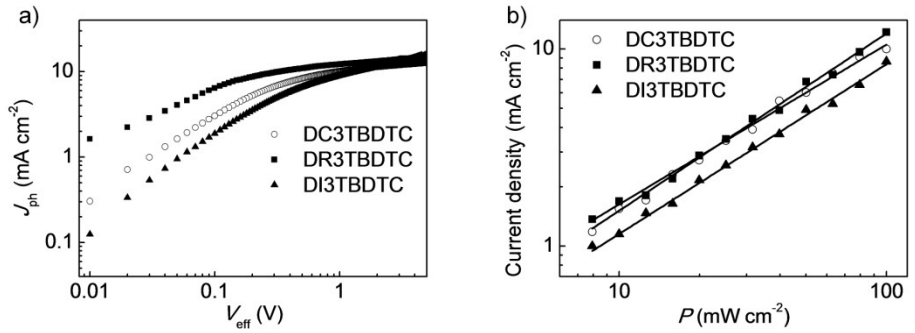

Figure S7. a) J_{ph} versus V_{eff} plots; b) dependence of J_{SC} on light intensity for OSCs based on DC3TBDTC:PBN-13, DR3TBDTC:PBN-13 and DI3TBDTC:PBN-13.

7. Photovoltaic properties of OSC devices based on DC3TBDTC, DR3TBDTC and DI3TBDTC blending with P-BNBP-fBT.

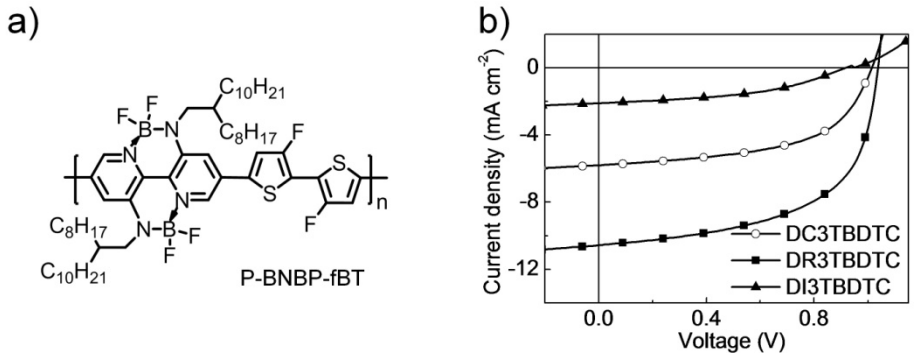

Figure S8. a) Chemical structures of P-BNBP-fBT. b) J-V curves of OSC devices based on donor:P-BNBP-fBT.

We used the efficient polymer acceptor P-BNBP-fBT (Adv. Mater. 2016, 28, 6504–6508) to fabricate OSC devices blending with these small molecule donors, which showed moderate to good performances.

Table S1. Photovoltaic performance of OSC devices based on donor: P-BNBP-fBT.

Donors	V_{OC} (V)	J_{SC} (mA/cm^2)	FF	PCE (%)

DC3TBDTC	1.01	5.81	0.56	3.28
DR3TBDTC	1.04	10.62	0.58	6.38
DI3TBDTC	0.92	2.11	0.44	0.85